

## Effect of Template Removal on Synthesis of Organic-Inorganic Hybrid Mesoporous MCM-48

Ya Nan Zhao, San Xi Li,<sup>†</sup> and Chong Soo Han<sup>\*</sup>

Department of Chemistry, Chonnam National University, Gwangju 500-757, Korea. \*E-mail: cshan@chonnam.ac.kr

<sup>†</sup>No. 111, Shenyang University of Technology, Shenyang West Road, Economic & Technological Development Zone, Shenyang, 110178, P.R. China

Received May 12, 2012, Accepted July 2, 2012

Post-synthesis is used to synthesize organic hybrid inorganic mesoporous sieves. In this method, the activity and structure of the base sieve are crucial to obtain the definable hybrid materials. The chemical and physical properties of the base can be largely changed either by the final step of its synthesizing processes, by template removal which is accomplished with the oxidative thermal decomposition (burning) method or by solvent extraction method. In this paper we compared two methods for the post-synthesis of organic hybrid MCM-48. When the template was extracted with HCl/alcohol mixture, the final product showed larger pore size, larger pore volume and better crystallinity compared to the case of the thermal decomposition. The reactivity of the surface silanol group of template free MCM-48 was also checked with an alkylsilylation reagent  $\text{CH}_2=\text{CHSi}(\text{OC}_2\text{H}_5)_3$ . Raman and  $^{29}\text{Si}$  NMR spectra of MCM-48 in the test reaction indicated that more of the organic group was grafted to the surface of the sample after the template was removed with the solvent extraction method. Direct synthesis of vinyl-MCM-48 was also investigated and its characteristics were compared with the case of post-synthesis. From the results, it was suggested that the structure and chemical reactivity can be maintained in the solvent extraction method and that organic grafting after the solvent extraction can be a good candidate to synthesize a definable hybrid porous material.

**Key Words :** MCM-48, Template removal, Reactivity of silanol group, Organic-inorganic hybrid

### Introduction

In the 1990's, various inorganic nano porous materials were investigated to provide a new application that departed from micro porous zeolites.<sup>1-3</sup> Of these nano porous materials, MCM-48 received attention because of its unique channel system showing two enantiomeric, bicontinuous, branched, self-intersecting volumes separated by an infinite wall running along the (100) and (111) directions forming a double gyroidal mesostructure with a three-dimensional network.<sup>4-6</sup> The development of the measuring instruments diverted our interest to the insight of the materials in nano scale and to the synthesis of a definable nano structure with a multi functional property. It was believed that the nano porous materials could be a good candidate to synthesize a definable hybrid porous material and the synthesis of organic-inorganic hybrid mesoporous material became essential.<sup>7</sup>

Mesoporous organic-inorganic hybrid silica are considered in potential applications in areas such as adsorption, chromatography, catalysis, sensor technology, and gas storage because of their large specific surface area and pore size with high coverage of introduced functional groups.<sup>8,9</sup> Post-synthesis grafting and direct co-condensation methods have generally used to modify the surface of mesoporous silica with organoalkoxysilanes,  $[(\text{R}'\text{O})_{4-n}\text{SiR}_{1-n}]_n$ ,  $n = 1-3$ .<sup>10</sup> Daehler *et al.*<sup>11</sup> examined the post-synthesis of  $\text{CH}_3$ -MCM-48 and  $\text{NH}_2$ -MCM-48, and found  $\text{CH}_3$ -functionalized material exhibited higher hydrolytic stability than unmodified MCM-

48, whereas  $\text{NH}_2$ -MCM-48 appeared to be less stable under the aqueous condition tested. Kumar *et al.*<sup>12</sup> obtained polyethyleneimine modified MCM-48 membranes by the solution growth method on symmetric R-alumina supports which showed higher selectivity to  $\text{N}_2$  permeation from the  $\text{N}_2/\text{CO}_2$  mixture in the presence of water vapor. Zhang *et al.*<sup>13</sup> synthesized amine functionalized porous catalysts by using an ultrasonic technique under a mild condition. Lim *et al.*<sup>14</sup> prepared vinyl-functionalized MCM-41 samples by a post-synthesis grafting process and a direct co-condensation method and compared the two methods. They observed that vinyl-grafted MCM-41 exhibited greater hydrothermal stability than the unmodified MCM-41 and was capable of absorbing nonpolar solvents from aqueous mixtures or emulsions. T. Yokoi *et al.*<sup>15</sup> synthesized an amino-functionalized 2D hexagonal structure MCM-41 *via* direct and post-synthesis grafting methods using organoalkoxy silanes. They reported that the interaction between the hydrophilic amino-organic fragment and the hydrophobic tail region of the surfactant strongly influences the formation of the silica micelle composite. He *et al.*<sup>16</sup> prepared vinyl-functionalized MCM-48 materials by both direct and post-synthesis grafting methods and found that the direct synthesized sample showed larger pore sizes and higher thermal stabilities than the grafting sample.

In the above studies, mesoporous sieves were usually synthesized by the surfactant-mediate synthesis method which consisted of the mixing of the elemental source of the

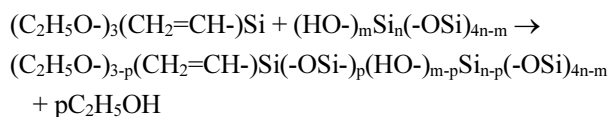
skeleton and the surfactant template, the growth of the skeleton around the template micelles and the removal of the template leaving the hollowed materials. In the synthesis of inorganic mesoporous materials such as M41S, simple burning (an oxidative thermal decomposition) of the organic template was used to remove the template. Since the burning method affected the reactivity of the surface by decomposed organics and the structure of the sieve, another method, for example the extraction of the template with a suitable solvent at a lower temperature, was tested.<sup>17</sup> Recently, the difference between the burning method and the solvent extraction method was demonstrated in a report on the gas flow through MCM-48 membranes on alumina.<sup>18</sup> Following the trend of the synthesis of organic-inorganic hybrid mesoporous materials, we attempted to understand the effect of the approaches in the base materials.

In this paper, we synthesized MCM-48 in a hydrothermal system under a wide mole ratio of  $n(\text{CTAB})/n(\text{TEOS})$  and compared the effect of the solvent extraction method and the oxidative thermal decomposition method on template removal. The chemical activity of the surface was investigated by a reaction of the silanol group with vinyltriethoxysilane  $[(\text{CH}_2=\text{CH})\text{Si}(\text{OC}_2\text{H}_5)_3]$ , (VTES). We also synthesized vinyl-MCM-48 *via* the co-condensation method using VTES and demonstrated the difference with the post-synthesis method.

## Experimental

**Synthesis of MCM-48.** A solution growth method was used to synthesize MCM-48 using molar composition of the reactants: 1.0 mol TEOS (tetraethyl orthosilicate): 0.45 mol CTABr (cetyltrimethyl ammonium bromide): 0.48 mol NaOH: 56 mol  $\text{H}_2\text{O}$ . TEOS was dropwise added under constant stirring of the mixed solution of CTABr and NaOH at room temperature for 3 h. The mixture was transferred to an autoclave and placed at 373 K for 72 h. The product was recovered by washing, filtering and drying at 353 K for 12 h. The template of as-synthesis MCM-48 was removed with heating at 823 K in air for 6 h (the thermal decomposition method) or extracting in  $\text{HCl}/\text{C}_2\text{H}_5\text{OH}$  solution at 353 K for 24 or 48 h (the solvent extraction method).

**Chemical Activity of MCM-48.** The reactivity of the surface silanol group of MCM-48 was investigated by a reaction with VTES. Typically, 0.5 g of dehydrated MCM-48 was dispersed in toluene while stirring at 343 K for 1 h. Then 8 mmol VTES was added and the mixture was stirred at 343 K for 24 h. The powder was collected by filtration, washed with ethanol and dried at 363 K for 12 h. It was assumed that silanol group(s) on the surface reacted with VTES and the vinylsilyl (or vinylsiloxy) group grafted on the surface as



where  $m = 1-3$ ,  $n = 1-3$  and  $p = 1-3$ .

**Synthesis of Vinyl-MCM-48.** The vinyl-MCM-48 was synthesized with the co-condensation method according to the referenced<sup>19</sup> and was modified as follows. Typically, the molar composition of the reactants was: 1.0 mol TEOS: 0.45 mol CTAB:  $z$  mol VTES: 0.48 mol NaOH: 56 mol  $\text{H}_2\text{O}$ , where  $0.00 \leq z \leq 0.25$ . VTES was added to the mixture after crystallization for 24 h and the total crystallization time was 72 h. The product was recovered by washing and filtering with distilled water. Then the template in the sample was removed with the solvent extraction. The solid was then filtered with ethanol and dried at 363 K for 12 h.

**Characterization of MCM-48.** Low-angle XRD patterns of MCM-48 were recorded on X'pert PRO Multi-Purpose X-Ray Diffractometer, PANalytical, Netherlands using  $\text{Cu-K}\alpha$  radiation ( $\lambda = 1.54060 \text{ \AA}$ ) with a step size of  $2\theta = 0.02^\circ$  and step scan time of 3 s. The Raman spectrometer was measured by Horiba LabRam HR800 (focal length of spectrometer = 80 cm), Horiba Jobin-Yvon, France. The pore size distribution, pore volume and surface area of the samples were determined by Micromeritics' ASAP 2020 Accelerated Surface Area and Porosimetry Analyzer. The morphology of the crystal was obtained on a Field Emission Scanning Electron Microscope (FE-SEM) using JSM-7500F+EDS (Oxford) JEOL Co., Japan. Solid state  $^{29}\text{Si}$  CP/MAS NMR spectra were performed by a 400 MHz solid state FT-NMR spectrometer (DSX 400 MHz), Bruker Analytische GmbH.

## Results and Discussion

**Synthesis of MCM-48.** MCM-48 was synthesized at the mole ratio of CTABr/TEOS of between 0.35 to 0.65. At the mole ratio of CTABr/TEOS of 0.45, the 3D cubic Ia3d MCM-48 was well formed after crystallization for more than 48 h. The effect of template removal methods was investigated with the sample synthesized from the molar composition of the reactants: 1.0 mol TEOS: 0.45 mol CTABr: 0.48 mol NaOH: 56 mol  $\text{H}_2\text{O}$  and crystallization at 373 K for 72 h.

The XRD patterns of the template free samples are shown in Figure 1. Sample SE (template removed with the solvent extraction for 48 h) showed strong peaks of (211), (220), (420), and (322) at  $2\theta = 2.377^\circ$ ,  $2.743^\circ$ ,  $4.287^\circ$ , and  $4.518^\circ$ , respectively. Sample TD (template removed with thermal decomposition for 6 h) displayed clear peaks of (211), (220), (420), and (332) at  $2\theta = 2.672^\circ$ ,  $3.081^\circ$ ,  $4.835^\circ$ , and  $5.091^\circ$ , respectively. For the sample after the solvent extraction method, the position of the (211) crystal plane was slightly increased compared to the as-synthesis sample ( $2\theta = 2.305^\circ$ ) which confirmed the preservation of the structure and pores. In the case of the thermal decomposition method, the peaks were moved to a higher position than the as-synthesis MCM-48 or the sample after the solvent extraction method. These results indicated that high temperature caused a contraction of the mesoporous channels. The similar result was reported for mesoporous SBA-15 silica, which was further utilized as a solid template for the synthesis of carbon nanofibers.<sup>20</sup>

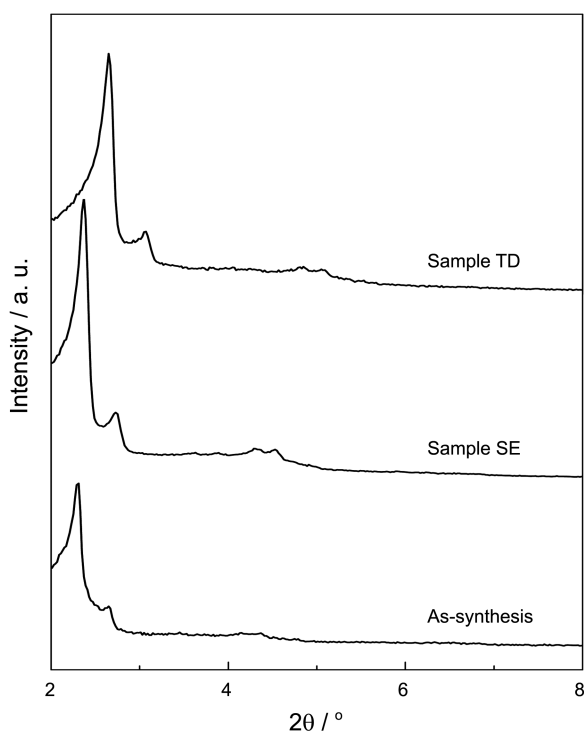


**Figure 1.** XRD patterns of MCM-48 (As-synthesis, template was not removed; Sample SE, template was removed with the solvent extraction for 48 h; Sample TD, template was removed with the thermal decomposition for 6 h).

MCM-48 has a dense framework structure and a periodic arrangement of pores. Thus, XRD can be used to give the information of periodic meso-porosity. The unit cell parameters and interplanar spacing which could be approximated to pore size were calculated from the position of the (211) peak using the Bragg equation and Cubic formula in Table 1. The unit cell parameter and interplanar spacing for the case of the solvent extraction method were larger than those for the case of the thermal decomposition method.

Figure 2 shows the Raman spectra of the as-synthesis and template removed MCM-48 with the solvent extraction for 24 h, the solvent extraction for 48 h and the thermal decomposition for 6 h. The Raman peaks at  $2860\text{ cm}^{-1}$  and  $2924\text{ cm}^{-1}$  (stretching vibrations of  $\text{CH}_2$  and  $\text{CH}_3$ ), and the Raman peak at  $1482\text{ cm}^{-1}$  (plane bending vibration of  $\text{CH}_2$ ) belong to the template reagent. The sample with solvent extraction for 24 h showed a small amount of template remaining while all the template was removed after the

**Table 1.** Unit cell parameters ( $a_0$ ) and interplanar spacing of MCM-48 calculated from XRD patterns. ( $a_0 = \sqrt{6} d_{211}$ , As-synthesis, template was not removed; Sample SE, template was removed with the solvent extraction for 48 h; Sample TD, template was removed with the thermal decomposition for 6 h)

Method	$2\theta$ (°)	$d_{211}$ (nm)	$a_0$ (nm)
As-synthesis	2.30	3.8	9.3
Sample SE	2.38	3.7	9.1
Sample TD	2.67	3.3	8.1

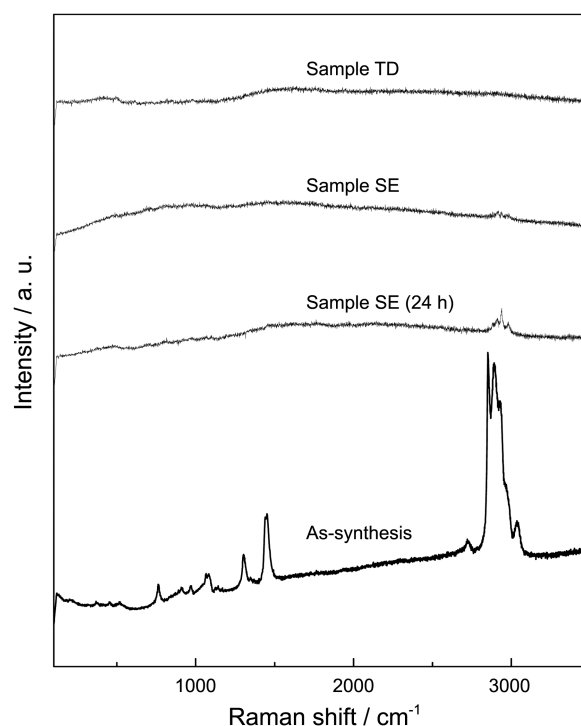


**Figure 2.** Raman spectra of MCM-48. (As-synthesis, template was not removed; Sample SE (24 h), template was removed with the solvent extraction for 24 h; Sample SE, template was removed with the solvent extraction for 48 h; Sample TD, template was removed with the thermal decomposition for 6 h).

thermal decomposition for 6 h (Sample TD) and after the solvent extraction for 48 h (Sample SE).

Figure 3 and Table 2 show the  $\text{N}_2$  adsorption-desorption isotherms and pore size distribution of the template removed MCM-48. The shape of curves was irreversible and exhibited a hysteresis loop (type IV), which was associated with the capillary condensation taking place in the mesopores.<sup>21</sup> Pore size distribution showed that the sample obtained from the solvent extraction method had larger pore size and pore volume than the thermal decomposition method. This result was consistent with the result of XRD.

Figure 4 showed the SEM image of the MCM-48 samples. Sample SE showed the aggregated and cambered structure of the crystalline particles. After the thermal decomposition method, the particles became more dispersed and irregular than after the solvent extraction method. This could be explained by the fact that the high temperature treatment caused a reduction of the physical congregation ability between the particles.

**Chemical Activity of MCM-48 Obtained from Different Template Removal Method.** Figure 5 shows the Raman spectra of MCM-48 reacted with VTES after template removal. VTES showed a peak at  $\sim 1604\text{ cm}^{-1}$  corresponding to the vibrations of  $(\text{Si})\text{-CH}=\text{CH}_2$ ; a peak at  $3064\text{ cm}^{-1}$  belonging to the stretching vibrations of  $=\text{C-H}$ ; a peak at  $675\text{-}1000\text{ cm}^{-1}$  considering the plane bending vibration of  $=\text{C-H}$ ; a peak at  $1407\text{ cm}^{-1}$  for the scissoring vibrations of  $-\text{CH}_2$ ;<sup>22</sup> peaks at  $2850\text{-}3000\text{ cm}^{-1}$  corresponding to the

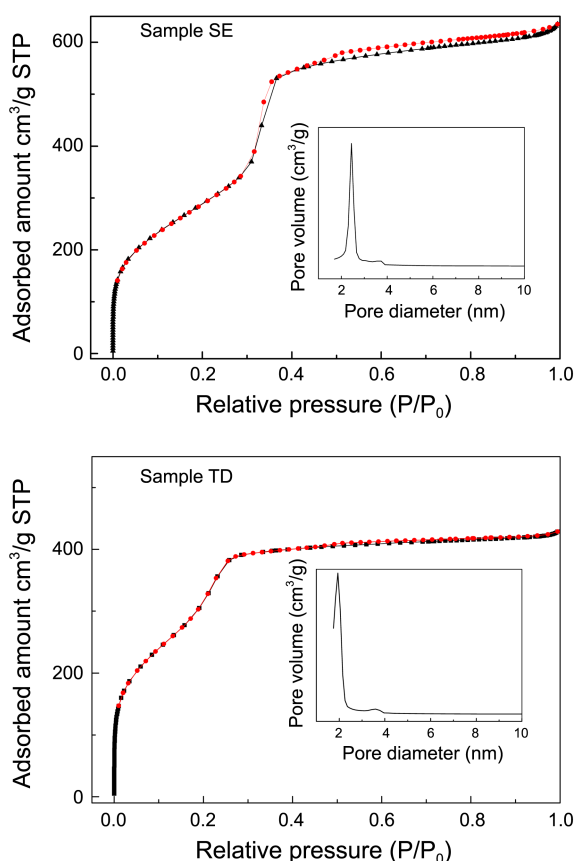


**Figure 3.**  $N_2$  adsorption/desorption isotherm and BJH pore size distributions of MCM-48 after the solvent extraction of template for 48 h (Sample SE) and after the thermal decomposition of template for 6 h (Sample TD).

**Table 2.** Structural properties of MCM-48 after the solvent extraction of template for 48 h (Sample SE) and the thermal decomposition of template for 6 h (Sample TD)

Method	$S_{BET}$ ( $m^2/g$ )	$V_p$ ( $cm^3/g$ )	Mean pore size (nm)
Sample SE	1070	0.98	2.7
Sample TD	1116	0.66	2.2

stretching vibrations of  $CH_2$  and  $CH_3$ ; and peaks at  $1100\text{ cm}^{-1}$  and  $1280\text{ cm}^{-1}$  corresponding to the  $-O-Si$  and  $SiC$  stretches.<sup>6,18</sup> When VTES reacted with the template removed MCM-48, the peaks of  $(Si)-CH=CH_2$ ,  $=C-H$ ,  $-O-Si$  and  $SiC$  were observed. This proved that the vinylsilyl groups were successfully grafted to the surface of MCM-48 after two different template removal methods. The vinylsilyl grafted MCM-48 after the solvent extraction method showed stronger absorption of the related Raman peaks than the thermal decomposition method. This meant that the MCM-48 obtained from the solvent extraction method showed higher concentration of reactive silanol than that obtained from the thermal decomposition method. This could be explained by the fact that the low temperature of the solvent extracted method maintained the active OH groups on the surface of MCM-48.

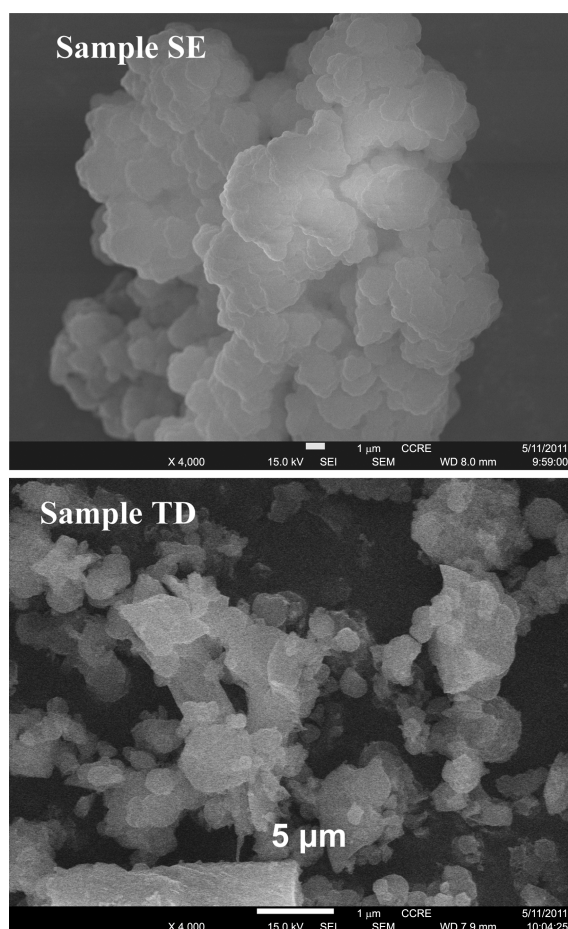


**Figure 4.** The SEM images of MCM-48 after the solvent extraction of template for 48 h (Sample SE) and the thermal decomposition of template for 6 h (Sample TD).

The solid-state  $^{29}Si$  CP/MAS NMR spectra of the template removed MCM-48 showed three distinct peaks at  $-91$  ppm,  $-101$  ppm and  $-110$  ppm as shown in Figure 6. These were assigned as the surface geminal silanol groups [ $Q_2$ ,  $Si(OH)_2(OSi)_2$ ], vicinal silanol groups [ $Q_3$ ,  $Si(OH)(OSi)_3$ ] and framework silica [ $Q_4$ ,  $Si(OSi)_4$ ], respectively.<sup>23,24</sup> The  $Q_4$  position of the sample obtained from the thermal decomposition,  $-111$  ppm, slightly shifted to the low field region compared to that of the solvent extraction,  $-110$  ppm, which indicated the more extensively cross-linked framework of the high temperature treated MCM-48 sample. The intensity of  $Q_2$  and  $Q_3$  decreased after vinylsilyl grafting, especially for the solvent extraction method. The increased intensity of  $Q_4$  indicated that a part of the  $Si-OH$  of  $Si(OH)_2(OSi)_2$  and  $Si(OH)(OSi)_3$  reacted with the VTES forming framework such as silica  $Si(OSi)_4$ . The NMR spectra of the vinylsilyl grafted MCM-48 significantly differed from that of MCM-48. Additional peaks at around  $-64$  ppm, at  $-71$  ppm, and at  $-80$  ppm corresponding to  $R(R'O)_2Si(-O-)$  [ $R=(CH_2=CH)$ ,  $R'=H$  or  $C_2H_5$ ],  $R(R'O)_2Si(-O-)$ , and  $RSi(-O-)_3$  were attributed to the surface-grafted species, which were marked as  $T_1$ ,  $T_2$ , and  $T_3$ , respectively. The  $(-O-)$  can represent either oxygen atoms of the silica surface or those of the adjacent

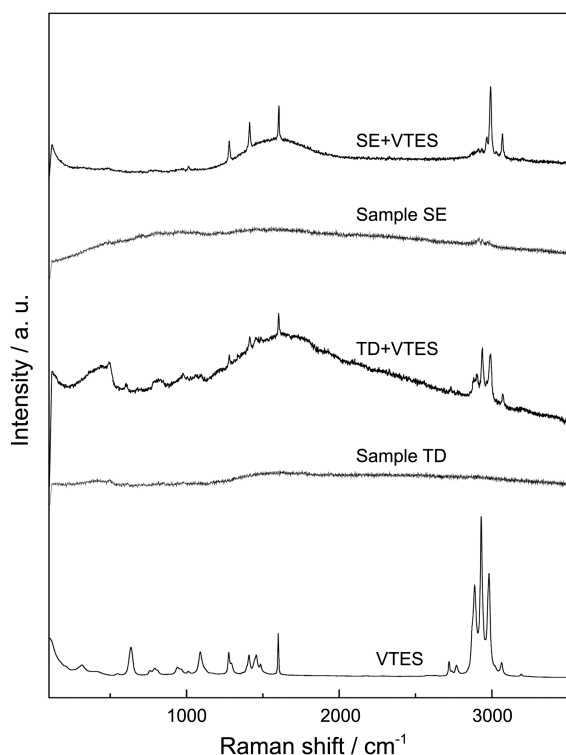


**Figure 5.** Raman spectra of MCM-48 (VTES, vinyltriethoxysilane; Sample SE, template was removed with the solvent extraction for 48 h; Sample TD, template was removed with the thermal decomposition for 6 h. TD+VTES, Sample TD after reaction with VTES; SE+VTES, Sample SE after reaction with VTES).

grafted centers.<sup>23</sup> NMR spectra proved that the vinylsilyl group was successfully grafted to MCM-48 and the sample after the solvent extraction was more reactive to VTES.

Table 3 shows the framework connectivities of samples determined by the <sup>29</sup>Si CP/MAS NMR spectra. The Q<sub>3</sub>/Q<sub>4</sub> and Q<sub>2</sub>/Q<sub>4</sub> ratios of the sample after the solvent extraction showed a slightly higher value than the thermal decomposition. This indicated that the thermal decomposition resulted in higher condensation of material framework or a higher polymerization of silica atoms than the solvent extraction.<sup>25</sup> The decreases in the Q<sub>2</sub>/Q<sub>4</sub> and Q<sub>3</sub>/Q<sub>4</sub> ratios of MCM-48 were observed after the reaction with VTES for both the cases of template removing methods while the

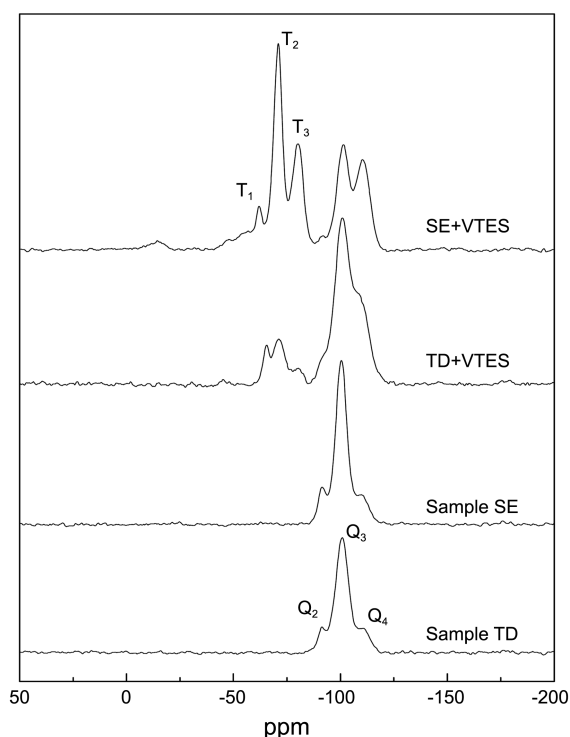


**Figure 6.** Solid-state <sup>29</sup>Si CP/MAS NMR spectra of MCM-48 (Sample SE, template was removed with the solvent extraction for 48 h; Sample TD, template was removed with the thermal decomposition for 6 h. TD+VTES, Sample TD after reaction with VTES; SE+VTES, Sample SE after reaction with VTES).

ratios for the solvent extraction method reduced more drastically. This could be explained by the fact that there were more reactive sites on the surface of MCM-48 after the solvent extraction compared to the thermal decomposition and VTES produced R(R'O)<sub>2</sub>Si(-O-), R(R'O)<sub>2</sub>Si(-O-) and RSi(-O)<sub>3</sub> moieties on the surface.<sup>26</sup>

#### Synthesis of Vinyl-MCM-48 by co-condensation Method.

The effect of mole ratio of VTES/TEOS on synthesized vinyl-MCM-48 (vinylsiloxy group inserted to MCM-48 skeleton) was studied using the crystallized time of 72 h and the addition of VTES to the mixture after crystallization for 24 h. Figure 7 shows the XRD patterns of the template free samples obtained at different amounts of VTES. The XRD

**Table 3.** The framework connectivities of MCM-48 determined by <sup>29</sup>Si CP/MAS NMR spectra (Sample SE, template was removed with the solvent extraction for 48 h; Sample TD, template was removed with the thermal decomposition for 6 h. TD+VTES, Sample TD after reaction with VTES; SE+VTES, Sample SE after reaction with VTES; Vinyl-MCM-48, synthesized by co-condensation method with mole ratio of VTES/TEOS = 0.10)

Chemical shift (ppm)	Sample TD	Sample SE	TD+VTES	SE+VTES	Vinyl-MCM-48
δ <sub>1</sub> (Q <sub>4</sub> )	-111	-110	-108	-110	-110
δ <sub>2</sub> (Q <sub>3</sub> )	-101	-100	-101	-101	-100
δ <sub>3</sub> (Q <sub>2</sub> )	-91	-91	-91	-91	-93
δ <sub>4</sub> (T <sub>3</sub> )	-	-	-80	-80	-79
δ <sub>5</sub> (T <sub>2</sub> )	-	-	-71	-71	-71
δ <sub>6</sub> (T <sub>1</sub> )	-	-	-66	-62	-64
Q <sub>2</sub> /Q <sub>4</sub>	0.78	0.90	0.17	0.08	0.45
Q <sub>3</sub> /Q <sub>4</sub>	6.32	6.69	2.07	1.09	4.27

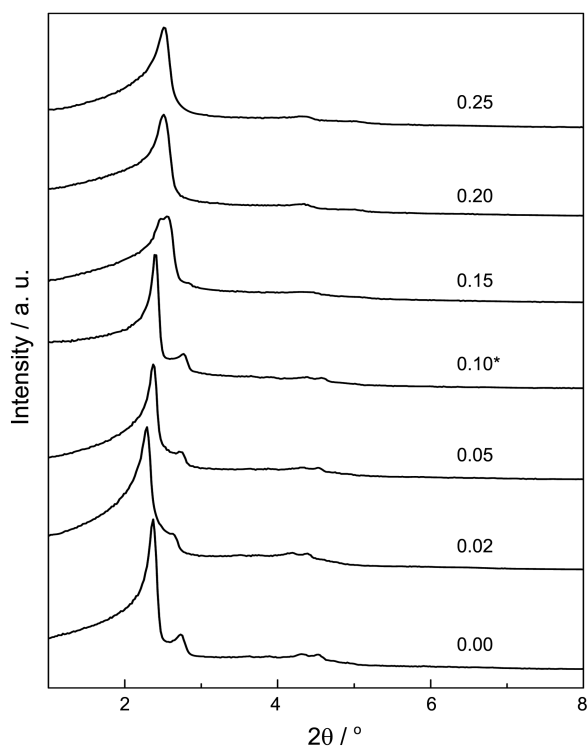


**Figure 7.** XRD spectra of vinyl-MCM-48 synthesized via co-condensation with different mole ratio of VTES/TEOS.

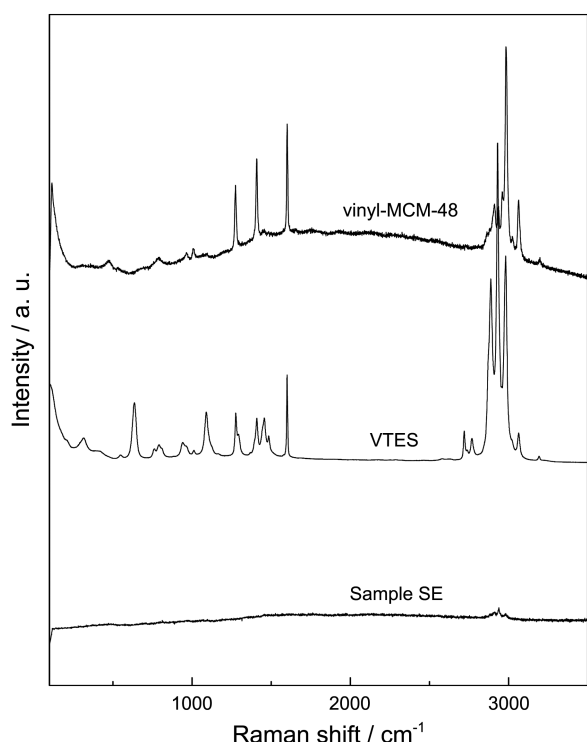


**Figure 8.** Raman spectra of vinyl-MCM-48 and MCM-48 (Sample SE, MCM-48 after solvent extraction of template for 48 h; VTES, vinyltriethoxysilane; vinyl-MCM-48, MCM-48 synthesized via co-condensation with mole ratio of VTES/TEOS = 0.10).

pattern showed that the vinyl-MCM-48, which had a 3D cubic structure, could be synthesized when the mole ratio of VTES/TEOS was  $\leq 0.10$ . The increased mole ratio of

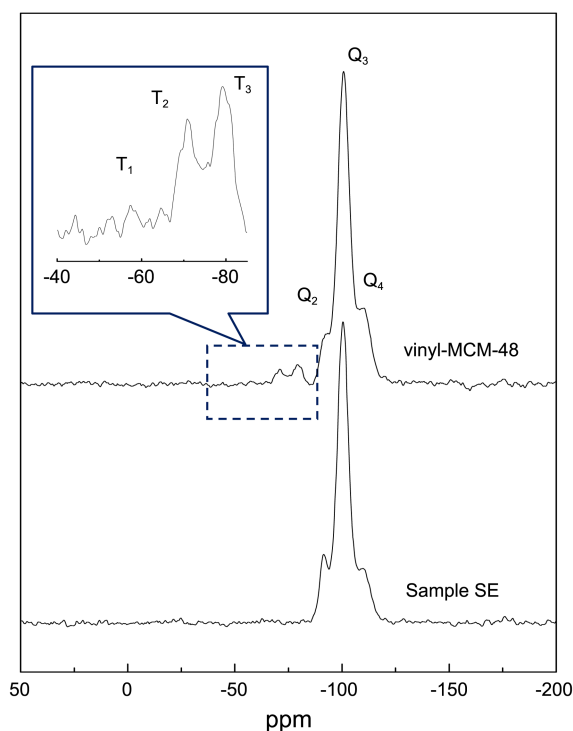


**Figure 9.** Solid-state  $^{29}\text{Si}$  CP/MAS NMR spectra of vinyl-MCM-48 and template free MCM-48 (Sample SE, MCM-48 after solvent extraction of template for 48 h; vinyl-MCM-48, MCM-48 synthesized via co-condensation with mole ratio of VTES/TEOS = 0.10).

VTES/TEOS to 0.15 resulted in the decrease of the intensity of the (220) crystal plane. With a further increase of the ratio, there were only (211) peaks left and the sample no longer belonged to the 3D cubic Ia3d mesophase MCM-48. Vinyl-MCM-48 was synthesized in a narrow mole ratio of VTES/TEOS ( $\leq 0.10$ ) via the co-condensation method because of the steric hindrance of the vinyl group. The observation showed the same trend as that in the report of Gaslain *et al.*<sup>27</sup> who synthesized mercaptopropyl-functionalized silica spherical particles of MCM-41 or MCM-48 by the co-condensation of MPTMS (mercaptopropyl trimethoxysilane) or MPTES (mercaptopropyl triethoxysilane) and TEOS precursors, where hexagonal or cubic mesoporous structures could be well-ordered only when synthesized with low amounts of MPTES (below 9%).

Raman spectra of template free MCM-48, VTES (liquid) and vinyl-MCM-48 are shown in Figure 8. Vinyl-MCM-48 showed strong peaks at  $1607\text{ cm}^{-1}$ ,  $1407\text{ cm}^{-1}$ ,  $1281\text{ cm}^{-1}$ ,  $3064\text{ cm}^{-1}$  and  $3205\text{ cm}^{-1}$  which were typical peaks of the vinyl group.<sup>18,28</sup> In addition, peaks of  $2800\text{--}3000\text{ cm}^{-1}$  corresponded to the stretching vibrations of  $\text{CH}_2$  and  $\text{CH}_3$  and peaks appeared at  $675\text{--}1000\text{ cm}^{-1}$  considering the plane bending vibration of  $=\text{C-H}$ .  $-\text{O-Si}$  and  $\text{SiC}$  stretchings at  $1100\text{ cm}^{-1}$  and  $1280\text{ cm}^{-1}$  were identified. Raman spectra proved that vinyl-MCM-48 were successfully synthesized by the co-condensation method at a mole ratio of VTES/TEOS of less than 0.10.

Figure 9 shows the solid-state  $^{29}\text{Si}$  CP/MAS NMR spectrum of vinyl-MCM-48 via the co-condensation method.

The vinyl-MCM-48 spectrum of the sample significantly differed to that of the unmodified MCM-48 (Sample SE). Small peaks of  $-64$  ppm,  $-71$  ppm, and  $-79$  ppm could be attributed to the surface species,  $R(R'O)_2Si(-O-)$ ,  $R(R'O)_2Si(-O-)$  and  $RSi(-O)_3$  for the case of vinylsilyl grafted samples, respectively. However, the intensities of the peaks,  $T_1$ ,  $T_2$  and  $T_3$  were considerably smaller than those of the previously described vinylsilyl grafted MCM-48.

The ratios of  $Q_3/Q_4$  and  $Q_2/Q_4$  of vinyl-MCM-48 via the co-condensation method are listed and compared to vinylsilyl grafted MCM-48 in Table 3. The lower  $Q_3/Q_4$  or  $Q_2/Q_4$  ratio compared to MCM-48 (Sample SE) was caused by the silane reagent inserted into the interspace of the micelles and increased the condensation of the material framework or the polymerization of silica atoms.

### Conclusions

The effect of the template removing methods on the reactivity of the surface of MCM-48 was investigated. The XRD pattern showed that there was little change of the  $2\theta$  position with the solvent extraction method, which confirmed the preservation in the structure and pore within the process.  $N_2$  adsorption also showed that the solvent extraction method resulted in a larger pore size and volume. The sample obtained with the solvent extraction method showed a higher concentration of reactive coupling sites on the surface than the thermal decomposition method in Raman and  $^{29}Si$  NMR measurements in a reaction with vinyltriethoxysilane. This was explained by the fact that the high temperature caused a contraction of silanol on the surface of mesoporous MCM-48 and reduced the active sites.

Raman and  $^{29}Si$  NMR spectra proved that vinyl-MCM-48 was successfully synthesized by the co-condensation of vinyl triethoxysilane (VTES) with tetraethyl orthosilicate (TEOS). The mole ratio of VTES/TEOS showing a 3D cubic structure in the XRD pattern was 0.00-0.10. Both the post-grafting method and the co-condensation method can be used to synthesise the surface modified mesoporous silica via the covalent bonding of organic groups. It is generally believed that the organic units distributed more homogeneously in the case of the co-condensation method than the post-grafting method.<sup>29</sup> This study showed that the post-grafting method would be a good candidate to synthesize definable organic hybrid mesoporous sieves if the template is removed with solvent extraction in the final step of the synthesis of the base.

**Acknowledgments.** This work was financially supported by Chonnam National University in 2011.

### References

- Corma, A.; Kan, Q.; Navarro, M. T.; Perez-Pariente, J.; Rey, F. *Chem. Mater.* **1997**, *9*, 2123.
- Kresge, A. C. T.; Leonowicz, M. E.; Roth, W. J.; Vaturi, J. C.; Beck, J. S. *Nature* **1992**, *359*, 710.
- Beck, J. S.; Vartuli, J. C.; Leonowicz, M. E.; Kresge, C. T.; Schemitt, K. D.; Chu, T.-W.; Olson, D. H.; Sheppard, E. W.; McCullen, S. B.; Higgins, J. B.; Schlenker, J. L. *J. Am. Chem. Soc.* **1992**, *114*, 10834.
- Kaneda, M.; Tsubakiyama, T.; Carlsson, A.; Sakamoto, Y.; Ohsuna, T.; Terasaki, O.; Joo, S. H.; Ryoo, R. *J. Phys. Chem. B* **2002**, *106*, 1256.
- Schumacher, K.; Ravikovitch, P. I.; Du Chesne, A.; Neimark, A. V.; Unger, K. K. *Langmuir* **2000**, *16*, 4648.
- Wohlgemuth, M.; Yufa, N.; Hoffman, J.; Thomas, E. L. *Macromolecules* **2001**, *34*, 6083.
- Asefa, T.; MacLachlan, M. J.; Coombs, N.; Ozin, G. A. *Nature* **1999**, *402*, 867.
- Hoffmann, F.; Cornelius, M.; Morell, J.; Froba, M. *Angew. Chem. Int. Ed.* **2006**, *45*, 3216.
- Zhao, X. S.; Lu, G. Q.; Zhu, H. Y. 24th Australia and New Zealand Chemical Engineering Conference and Exhibition **1996**, *4*, 39.
- Sayari, A.; Hamoudi, S. *Chem. Mater.* **2001**, *13*, 3151.
- Daehler, A.; Boskovic, S.; Gee, M. L.; Separovic, F.; Stevens, G. W.; O'Connor, A. J. *J. Phys. Chem. B* **2005**, *109*, 16263.
- Kumar, P.; Kim, S.; Ida, J.; Gulians, V. V. *Ind. Eng. Chem. Res.* **2008**, *47*, 201.
- Zhang, X.; Cui, W.; Han, W.; Zhang, Y.; Liu, S.; Mu, W.; Chang, Y.; Hu, R. *React. Kinet. Catal. Lett.* **2009**, *98*, 349.
- Lim, M. H.; Stein, A. *Chem. Mater.* **1999**, *11*, 3285.
- Yokoi, T.; Yoshitake, H.; Tatsumi, T. *J. Mater. Chem.* **2004**, *14*, 951.
- He, J.; Shen, Y. B.; Evans, D. G. *Microporous Mesoporous Mater.* **2008**, *109*, 73.
- Lim, M. H.; Blanford, C. F.; Stein, A. *J. Am. Chem. Soc.* **1997**, *119*, 4090.
- Kumar, P.; Ida, J.; Kim, S.; Gulians, V. V.; Lin, J. Y. S. *J. Memb. Sci.* **2006**, *279*, 539.
- Zhao, W.; Li, Q.; Wang, L.; Chu, J. L.; Qu, J. K.; Li, S. H.; Qi, T. *Langmuir* **2010**, *26*, 6982.
- Yoon, S. B.; Kim, J. Y.; Kooli, F.; Lee, C. W.; Yu, J. S. *Chem. Commun.* **2003**, 1740.
- Kleitz, F.; Be rube, F.; Guilet-Nocolas, R.; Yang, C.-M.; Thommes, M. *J. Phys. Chem.* **2010**, *114*, 9344.
- Ayed, L.; Chaieb, K.; Cheref, A.; Bakhrouf, A. *World J. Microbiol. Biotechnol.* **2009**, *25*, 705.
- Ma, H.; He, J.; Evans, D. G.; Duan, X. *J. Mol. Catal. B: Enzym.* **2004**, *30*, 209.
- Daehler, A.; Boskovic, S.; Gee, M. L.; Separovic, F.; Stevens, G. W.; O'Connor, A. J. *J. Phys. Chem. B* **2005**, *109*, 16263.
- Chen, X.; Huang, L.; Li, Q. *J. Phys. Chem. B* **1997**, *101*, 8460.
- Yuranov, I.; Moeckli, P.; Suvorova, E.; Buffat, P.; Minsker, L. K.; Renken, A. *J. Mol. Catal. A: Chem.* **2003**, *192*, 239.
- Gaslain, F. O. M.; Delacote, C.; Walcarius, A.; Lebeau, B. *J. Sol-Gel Sci. Technol.* **2009**, *49*, 112.
- Lim, M. H.; Blanford, C. F.; Stein, A. *J. Am. Chem. Soc.* **1997**, *119*, 4090.
- Pereira, C.; Alves, C.; Monteiro, A.; Magen, C.; Pereira, A. M.; Ibarra, A.; Ibarra, M. R.; Tavares, P. B.; Araujo, J. P.; Blanco, G.; Pintado, J. M.; Carvalho, A. P.; Pires, J.; Pereira, M. F. R.; Freire, C. *ACS Appl. Mater. Interfaces* **2011**, *3*, 2289.